

# Effect of scatter correction on image quality of digital breast tomosynthesis

Taewon Lee<sup>a</sup>, Jiseoc Lee<sup>a</sup> and Seungryong Cho<sup>a</sup>

<sup>a</sup>Nuclear & Quantum Engineering, KAIST

In cone-beam CT (CBCT) or tomosynthesis that uses a large area flat-panel detector, scatter from the object can degrade image quality substantially. A variety of scatter correction methods have been developed that show their own cons and pros. In this work, we used a fast and simple scatter correction method for digital breast tomosynthesis (DBT) and evaluated the effect of scatter correction on the image quality. Since the density and thickness of a breast in DBT scans is fairly uniform, we assumed scatter can be estimated by taking convolution of the primary data with a scatter kernel. We used a gaussian kernel with its amplitude and width empirically determined from other work. To evaluate the image quality, we used a detectability of a mass based on a prewhitening ideal observer. The experimental result shows 6% increase of the detectability after the scatter correction.

**Keywords:** Digital Breast Tomosynthesis, Scatter, Kernel, Deconvolution, Detectability

## 1. Introduction

X-ray scatter is a major cause of image quality degradation in DBT or in CBCT. Various scatter correction methods have been developed and reported: a deconvolution method that uses a scatter kernel to remove scatter from the measured data, a method that uses an opaque material to estimate scatter fluence, a method that uses Monte Carlo simulation, etc [1,2,3]. Since the density and thickness of a breast in DBT scans is fairly uniform, a single scatter kernel can be assumed to work reasonably well [1]. In this preliminary, we used a gaussian kernel with its amplitude and width empirically determined from our earlier work.

## 2. Materials and Methods

### 2.1 Scatter correction

In this study, the CIRS phantom was used to demonstrate the effect of scatter correction in DBT. We acquired data using a prototype DBT system. As shown in Fig.1, a projection was deconvolved by a gaussian kernel having width of 14mm at half-maximum and height of 2.5.

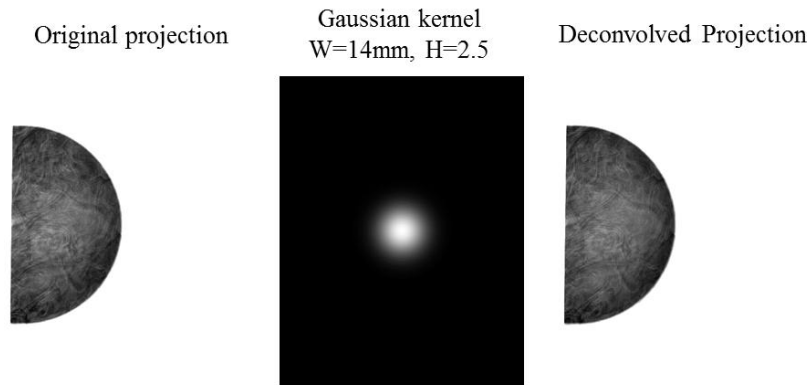


Figure 1. Projection images: before (left) and after (right) deconvolution.

Mathematical model of the deconvolution is as follows [2].

$$I_p = F^{-1} \left( \frac{F(I_m)}{F(\delta + g_s)} \right)$$

The measured projection data ( $I_m$ ) can be written as the sum of primary data ( $I_p$ ) and scatter data ( $I_s$ ). The scatter kernel is denoted by  $g_s$ , and  $\delta$  denotes a delta function.  $F$  refers to a Fourier transform and  $F^{-1}$  an inverse Fourier transform, respectively.

## 2.2 Total-variation minimization algorithm

For image reconstruction of DBT, we used a total-variation minimization (TV) algorithm. The TV algorithm seeks a solution that satisfy data consistency and nonnegativity with minimum image total-variation. Strategy of the TV algorithm is shown in the following [4].

$$\vec{f}^* = \operatorname{argmin} \|\vec{f}^*\|_{TV}$$

which satisfies two constraints,

$$|\vec{g}^c - M\vec{f}^*| < \epsilon \quad \text{and} \quad f_i \geq 0$$

$\epsilon$  can be selected for controlling the impact level of data inconsistency on the image reconstruction.

## 2.3 Detectability

We evaluated image quality using a prewhitening (PW) observer of a reconstructed mass in the CIRS breast phantom. We used a detectability of signals in complex backgrounds. The detectability square is defined as following [5].

$$d'^2 = \sum_k \frac{|S(k)|^2}{P_c(k)}$$

, where  $S(k)$  is Fourier transform of mass signal,  $P_c(k)$  is the noise power spectrum acquired from the background.

## 3. Results

In Fig. 2, we present line profiles of the projection data before and after the scatter correction. As can be seen, the projection data after the scatter correction has lower values than before, which is due to reduced amount of scatter contribution.

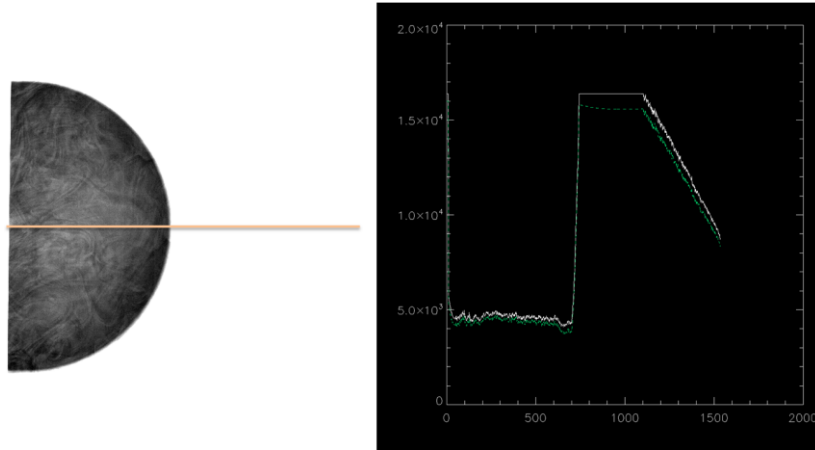


Figure 2. Example of projection data (left) and line profiles (right): before (solid line) and after (dashed line) scatter correction.

The reconstructed slice images are shown in Fig. 3. The image reconstructed from scatter-corrected data appears slightly brighter than the image reconstructed from uncorrected data. The detectability of a mass has increased by 6 % after the scatter correction.

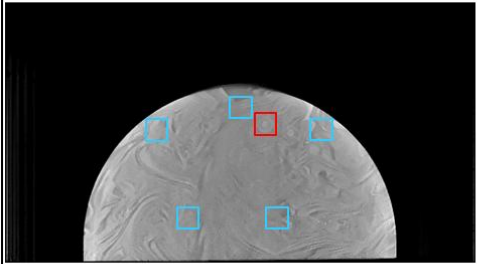
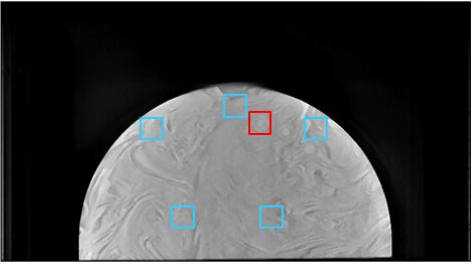
Uncorrected image	Corrected image
	
<b>Detectability : 35.3</b>	<b>Detectability : 37.4</b>

Figure 3. Reconstructed images from uncorrected (left) and from corrected (right) data.

#### 4. Discussion

In this study, instead of using contrast-to-noise ratio (CNR) which is classically widely used image quality metric, we used a detectability based on a PW observer to incorporate complex background noise more appropriately. As we assumed, a single scatter kernel seems to work reasonably well in DBT. A systematic study using advanced scatter kernels remains as our future work.

#### 5. Conclusions

We have applied a scatter correction method in DBT, and successfully demonstrated that the scatter correction improved the image quality.

#### References

1. J. A. Seibert, J. M. Boone. X-ray scatter removal by deconvolution. *Medical Physics* 1988;15;567-575
2. J L Ducote and S Molloy. Scatter correction in digital mammography based on image deconvolution. *Physics In Medicine And Biology*. 2010;55;1295-1309
3. David G. Kruger, Frank Zink, Walter W. Pepler, David L. Ergun, Charles A. Mistretta. A regional convolution kernel algorithm for scatter correction in dual-energy images: Comparison to single-kernel algorithm. *Medical Physics* 1994;21;175-184
4. Emil Y. Sidky, Chien-Min Kao, Xiaochuan Pan. Accurate image reconstruction from few-views and limited-angle data in divergent-beam CT. *Journal X-Ray Science and Technology* 2006;14;119-139
5. I. Reiser, R.M. Nishikawa. Task-based assessment of breast tomosynthesis: Effect of acquisition parameters and quantum noise. *Medical Physics* 2010;37;1591-1600